Relative stabilities of adsorbed versus substitutional Al atoms in submonolayer Al/Si_xGe_{1-x}(111)

D. V. Gruznev,[1] D. A. Olyanich,[1] D. N. Chubenko,[1] Yu. V. Luniakov,[1] I. A. Kuyanov,[1,2] A. V. Zotov,[1,2,3] and A. A. Saranin[1,2]

[1]*Institute of Automation and Control Processes, 690041 Vladivostok, Russia*

[2]*Faculty of Physics and Engineering, Far Eastern State University, 690000 Vladivostok, Russia*

[3]*Department of Electronics, Vladivostok State University of Economics and Service, 690600 Vladivostok, Russia*

(Received 23 May 2008; revised manuscript received 14 September 2008; published 8 October 2008)

Using scanning tunneling microscopy, low-energy electron-diffraction observations, and density-functional calculations, the effect of adding Ge to Si(111) substrate on the reconstructions induced by Al adsorption has been studied. It has been found that Ge incorporation alters the relative stability of the reconstructions. In particular, while in the "pure" Al/Si(111) system the magic cluster array (α-7×7 phase) is less stable than the $\sqrt{3}\times\sqrt{3}$ reconstruction (to which it irreversibly converts upon heating above 600 °C), in the Al/Si_xGe_{1-x}(111) system magic clusters possess an enhanced thermal stability and persist almost up to the Al desorption temperature of ~800°. The results of calculations allow us to track the sequential stages of the substitution of Si atoms by Ge in the α-7×7 phase. The general trend found is that adding Ge to Si(111) makes the Al substitutional configuration more preferable than the Al adatom configuration, which is opposite to the relative stabilities of the configurations in the pure Al/Si(111) system.

DOI: 10.1103/PhysRevB.78.165409 PACS number(s): 68.35.−p, 68.43.−h, 68.37.Ef, 61.05.jh

I. INTRODUCTION

Adsorbate-induced reconstructions on the surfaces of single-crystalline elemental semiconductors, Si and Ge, have been the object of numerous investigations for the last 50 years.[1,2] At present, they receive still increasing interest motivated by technological importance for nanoengineering. Understanding which specific parameters of the substrate surface and adsorbate overlayer control the structure and properties of a given reconstruction and finding techniques to alter them in a desired way are the challenging tasks for researchers. Among the most promising approaches to reach the goal is the one associated with controllable change in a system composition. Within this approach, adding the second adsorbate is a rather traditional technique which has been successfully used for many years. Less abundant is a technique based on the modification of a substrate surface. In case of the Si substrates, this is adding Ge, which is chemically akin to Si but has 4% larger lattice constant. As the initial adsorption of Ge onto the Si substrate is displacive, a homogeneously mixed Ge_xSi_{1-x} alloying layer can be formed on the Si substrate.[3–7] A surface of this layer is believed to be a fascinating playground for observing interesting phenomena related to the reconstruction formation as the main effect produced by adding Ge is just changing (increasing) the mean lattice constant of the substrate.

In our previous study,[8] we have examined the In/Ge_xSi_{1-x}(111) system and detected reconstructions, 7×3 and $\sqrt{21}\times\sqrt{21}$, which are not observed in the "pure" In/Si(111) and In/Ge(111) systems. The object of the present study was a ~0.3 monolayer (ML) of Al adsorbed onto the Ge_xSi_{1-x}(111) surface. We have found that all the reconstructions well known for the Al/Si(111) system, $\sqrt{3}\times\sqrt{3}$, $\sqrt{7}\times\sqrt{7}$, magic cluster array (α-7×7 phase), and γ phase, are preserved at the Ge_xSi_{1-x}(111) surface but their relative stability alters dramatically. Particular sequence of this effect is the enhanced thermal stability of the magic cluster array. Bearing in mind the promising properties of the magic clusters,[9] in particular those of an effective catalyst,[10] the enhanced stability could facilitate their prospective applications.

II. EXPERIMENTAL AND CALCULATION DETAILS

Our experiments were performed with Omicron scanning tunneling microscope (STM) operated in an ultrahigh vacuum ($\sim2.0\times10^{-10}$ Torr). Atomically clean Si(111)7×7 surfaces were prepared *in situ* by flashing to 1280 °C after the samples were first outgassed at 600 °C for several hours. Aluminum was deposited from an Al-wrapped W filament at a rate of 0.20 ML/min. [1 ML=7.8×10^{14} cm^{-2}, top Si atom density on the unreconstructed Si(111)1×1 surface]. Germanium was deposited from a W basket at a rate of 0.25 ML/min. For STM observations, electrochemically etched tungsten tips cleaned by *in situ* heating were employed. The STM images were acquired in a constant-current mode after cooling the sample to room temperature (RT).

To find the energetically favorable structures among the possible ones, we performed *ab initio* total-energy calculations using the FHI96MD code,[11] in which the Car-Parrinello type of electronic structure calculations[12] was used. The local-density approximation after Ceperley and Alder[13] in the Perdew-Zunger parametrization[14] for the exchange and correlation functional and fully separable Hamann[15] pseudopotentials has been employed. The pseudopotentials were constructed using the FHI98PP code[16] and were verified to avoid ghost states and to describe the basic experimental characteristic of bulk materials.

The surface has been simulated by a periodic slab geometry with 1×1, $\sqrt{3}\times\sqrt{3}$, and 7×7 unit cells containing eight (for 1×1 and $\sqrt{3}\times\sqrt{3}$) and four (for 7×7) silicon atomic layers. The dangling bonds of the bottom slab layer have been saturated by hydrogen atoms. The hydrogen atoms and bottom layer silicon atoms have been fixed and the rest at-

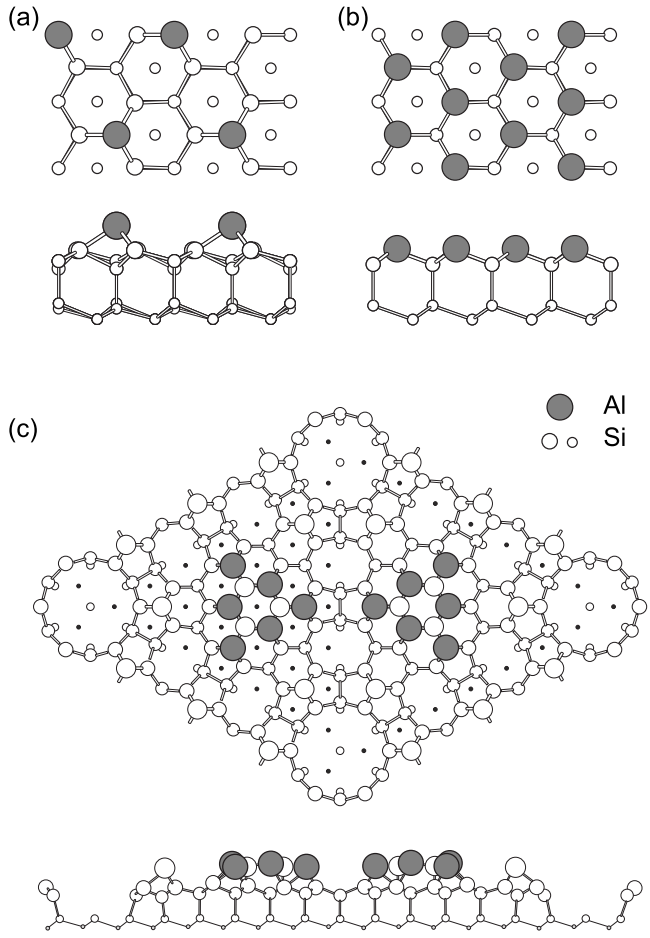

FIG. 1. Schematic illustrating various atomic configurations (top and side views) of Al adsorbate on the Si(111) surface including (a) adatom configuration (as in the $\sqrt{3}\times\sqrt{3}$ phase), (b) sustitutional configuration (as in the interior of the domains of the γ phase), and (c) surface magic clusters (as in the α-7×7 phase).

oms have been set free to move. A vacuum region of approximately 10 Å has been incorporated within each periodic unit cell to prevent interaction between adjacent surfaces. The energy cutoff of 13 Ry has been applied in all calculations presented.

III. RESULTS AND DISCUSSION

A. Al/Si(111) and Al/Ge(111)

Before considering Al adsorption onto the $Ge_xSi_{1-x}(111)$ surface, let us review briefly the reconstructions formed in the pure submonolayer Al/Si(111) and Al/Ge(111) systems. Upon Al deposition onto the Si(111)7×7 surface held at relatively high temperatures of ~650–750 °C, the $\sqrt{3}\times\sqrt{3}$, $\sqrt{7}\times\sqrt{7}$, and γ phase sequentially form.[17] The $\sqrt{3}\times\sqrt{3}$-Al phase is made of Al adatoms, which reside in T_4 sites of the almost bulklike Si(111) surface [see Fig. 1(a)]. Ideally, it contains 1/3 ML of Al, but actually the most homogeneous Si(111)$\sqrt{3}\times\sqrt{3}$-Al surface has been found to contain 0.25 ML of Al adatoms and 0.08 ML of Si adatoms.

The Si(111)$\sqrt{7}\times\sqrt{7}$-Al phase consists of Al adatoms located about T_4 sites forming the trimers with the centers in the on-top sites.[18] An Al coverage in the $\sqrt{7}\times\sqrt{7}$-Al reconstruction is 3/7 ML (one trimer per $\sqrt{7}\times\sqrt{7}$ unit cell). Typically, domains of the $\sqrt{7}\times\sqrt{7}$-Al phase coexist with the domains of the other Al/Si(111) reconstructions.

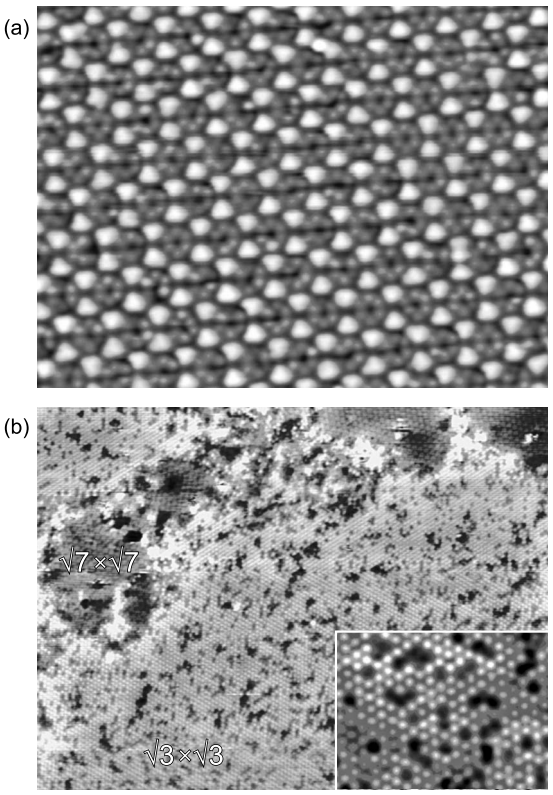

FIG. 2. Irreversible structural transition of the α-7×7-Al phase to the $\sqrt{3}\times\sqrt{3}$ reconstruction taking place in the Al/Si(111) system upon heating above 600 °C. (a) 295×220 Å^2 filled-state (−2.8 V) STM image of the original magic cluster array (α-7×7-Al phase) prepared by depositing ~0.3 ML of Al onto Si(111)7×7 substrate at 550 °C. (b) 920×725 Å^2 empty-state (+1.9 V) STM image of the same surface after annealing above 600 °C. The surface comprises the extended $\sqrt{3}\times\sqrt{3}$ arrays with inclusions of the $\sqrt{7}\times\sqrt{7}$ reconstruction. Inset illustrates STM appearance (empty state, +2.0 V) of the $\sqrt{3}\times\sqrt{3}$ phase shown at a greater magnification (scale: 115×85 Å^2).

The Al/Si(111) γ phase[17,19–23] is formed upon saturated adsorption of ~0.65–0.75 ML of Al, which substitutes for the Si atoms in the outermost atomic layer of the bulklike Si(111)1×1 surface [Fig. 1(b)]. Due to a greater atomic radius of Al as compared to Si, incorporation of Al atoms leads to the increase in the surface lattice constant by ~10%. The misfit between the Al-incorporated layer and the Si bulk is relieved through the formation of a domain-wall net, which decomposes the surface into quasiperiodic incommensurate superlattice of triangle-shaped domains. The domains have close but not identical sizes; hence, the surface is lacking a well-defined long-range ordering. The periodicity of the γ-phase superstructure is associated with the mean size of the triangular subunits, which is ~9–10 [expressed in the units of the Si(111)1×1 lattice constant $a_0^{Si}=3.84$ Å].

The Si(111)α-7×7-Al phase [Fig. 2(a)] develops upon Al deposition at temperatures ranging from 475 to 600 °C. This

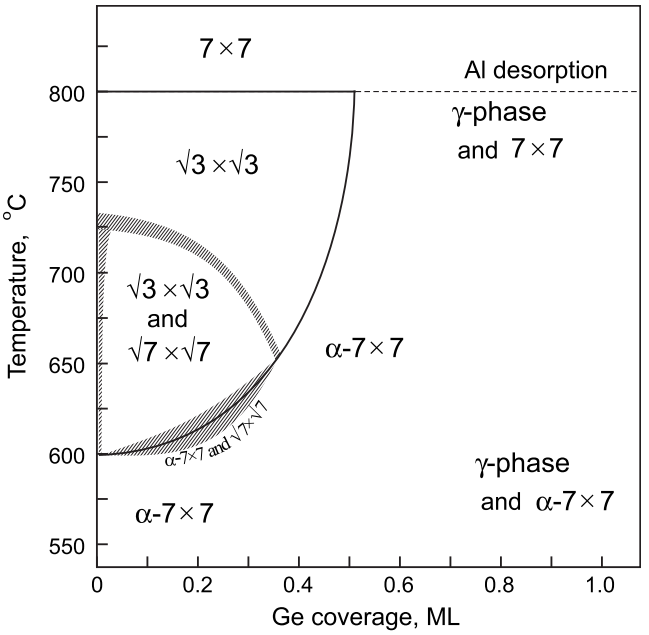

FIG. 3. Phase diagram illustrating effect of adding Ge to the Si(111) substrate on the surface structures observed by LEED in the system of ~0.3 ML of Al on $Ge_xSi_{1-x}(111)$ surface.

phase has recently been recognized as being essentially a highly ordered superlattice of the identical-size Al nanoclusters (magic clusters) on the Si(111)7×7 surface.[24,25] Each cluster consists of six Al atoms linked through three Si atoms to form a triangle-shape configuration with satisfied bonding [Fig. 1(c)]. Aluminum coverage in the ideal cluster array is $12/49 \simeq 0.24$ ML, but actually it is greater (~0.30 ML) due to substitution of about half of the corner Si adatoms by Al. The α-7×7-Al phase is metastable.[24,26,27] Upon heating above 600 °C it converts irreversibly into the $\sqrt{3}\times\sqrt{3}$ array with inclusions of the $\sqrt{7}\times\sqrt{7}$ reconstruction as illustrated in Fig. 2(b).

Compared to Al/Si(111), submonolayer Al/Ge(111) system is much less studied. To our knowledge, there is a single publication on this subject[28] where low-energy electron-diffraction (LEED) observation of the 2×2 and 10×10 reconstructions was reported. The 2×2 reconstruction is stabilized by the Al impurity, while the 10×10 formed by annealing several Al monolayers at ~650 °C is an incommensurate phase which is plausibly akin the Al/Si(111) γ phase.

B. Al/Ge_xSi_{1-x}(111): LEED and STM observations

The main regularities of the phase formation in the system of ~0.3 ML of Al on $Ge_xSi_{1-x}(111)$ surface are illustrated in the "phase diagram" shown in Fig. 3. For construction of the phase diagram, the following procedure was employed. First, a particular $Ge_xSi_{1-x}(111)$ surface was prepared by depositing a given amount of Ge (indicated in the ordinate axis of the diagram) onto the Si(111)7×7 surface at RT followed by annealing at 550 °C. Typically, the resultant surface displays a mixture of the 7×7 and 5×5 reconstructions with the 7×7 reconstruction prevailing. Then, ~0.3 ML of Al was deposited onto this surface at RT and the sample was annealed isochronally for 15 s at each temperature starting from 550 °C and up to Al desorption at 800 °C with a step of temperature increment being ~13 °C. Evolution of the surface structure was monitored by LEED after cooling the sample to RT. The result of each experimental run is a set of points along a vertical line at a fixed Ge coverage. The runs were conducted every 0.1 ML of Ge. Usage of the LEED observations ensures that domains of the phases indicated in the diagram are of relatively large size and occupy considerable surface area. STM observations were conducted for the points in the phase diagram which are of interest.

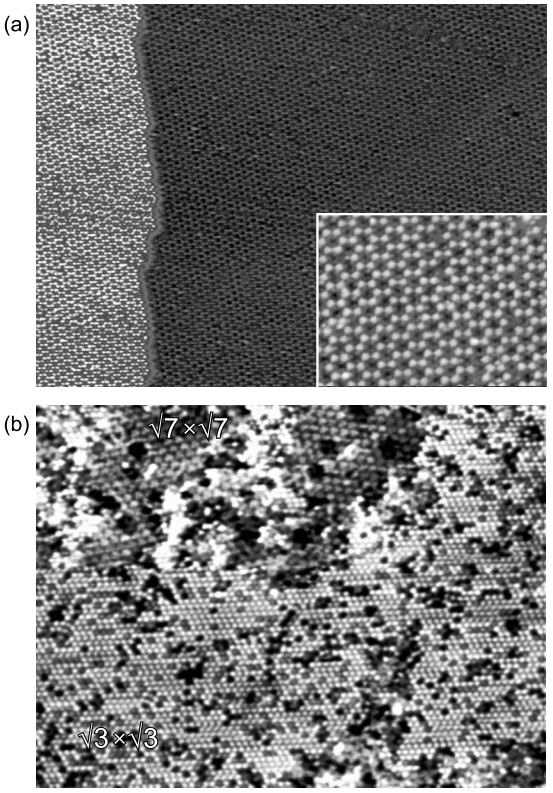

FIG. 4. (a) Large-scale (2.000×1.500 $Å^2$) filled-state (−2.2 V) STM image of the almost ideal magic cluster lattice (α-7×7-Al phase) formed in the Al/$Ge_xSi_{1-x}(111)$ system with 0.2 ML of Ge. Inset shows the surface at a greater magnification (scale: 450×270 $Å^2$). (b) 550×400 $Å^2$ empty-state (+1.7 V) STM image of the same surface after annealing at 675 °C. Like the case of the pure Al/Si(111) system, the surface comprises the $\sqrt{3}\times\sqrt{3}$ arrays with inclusions of the $\sqrt{7}\times\sqrt{7}$-reconstructed domains.

We have found that upon adding up to ~0.5 ML of Ge the α-7×7 phase (i.e., magic cluster superlattice) preserves the structure and it appears in STM images [see Fig. 4(a)] identical to the α-7×7 phase in the pure Al/Si(111) system. Similarly, annealing to high temperatures converts it to the $\sqrt{3}\times\sqrt{3}$ surface with inclusions of the $\sqrt{7}\times\sqrt{7}$ domains [Fig. 4(b)]. The difference is the greater transition temperature which grows with the Ge coverage. At ~0.5 ML of Ge, the α-7×7 phase persists almost up to Al desorption [i.e., at temperatures ~150 °C beyond the stability range of the pure α-7×7 Al/Si(111) phase].

Due to enhanced stability of the α-7×7 phase in the Al/$Ge_xSi_{1-x}(111)$ system, it can be produced by adding Ge

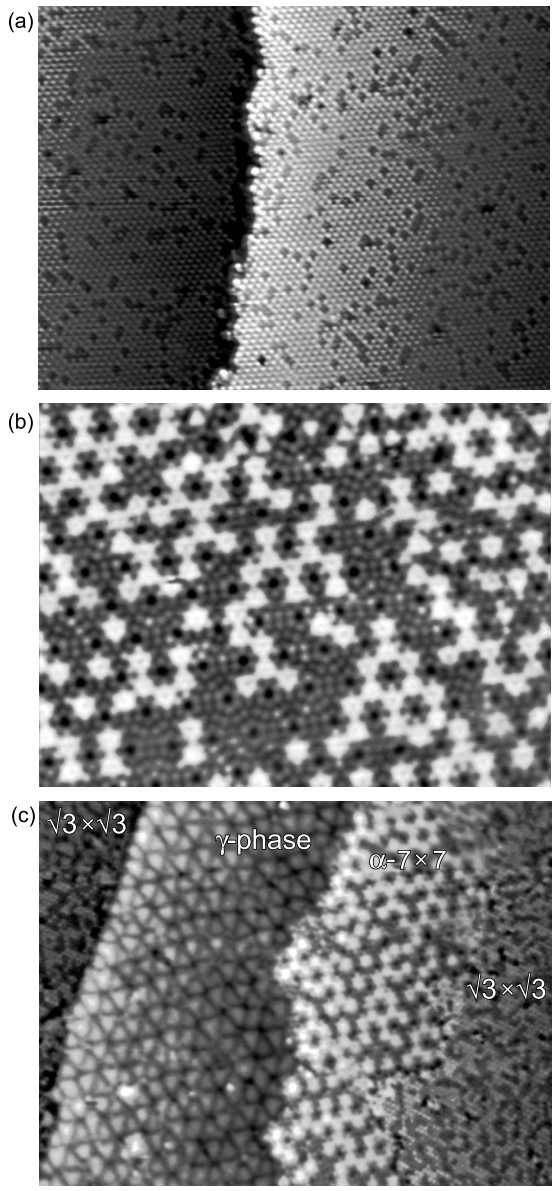

FIG. 5. Ge-induced transition from the $\sqrt{3}\times\sqrt{3}$ reconstruction to α-7×7 and γ phases. (a) 500×370 Å^2 empty-state (+1.85 V) STM image of the original $\sqrt{3}\times\sqrt{3}$-Al surface prepared by depositing ~0.25 ML of Al onto the Si(111)7×7 substrate at 700 °C. (b) 335×250 Å^2 empty-state (+3.1 V) STM image of the uncompleted magic cluster array (α-7×7 phase) formed by adding 0.5 ML of Ge at 500 °C to the $\sqrt{3}\times\sqrt{3}$-Al surface shown in (a). (c) Coexisting surface structures developed near the step edge upon adding 0.5 ML of Ge to the $\sqrt{3}\times\sqrt{3}$-Al surface at 400 °C. The regions occupied by the $\sqrt{3}\times\sqrt{3}$ reconstruction, α-7×7 phase, and γ phase are indicated.

to the $\sqrt{3}\times\sqrt{3}$-Al reconstruction. In other words, adding Ge can induce a structural transformation opposite to that in the pure Al/Si(111) system. This possibility is demonstrated in the experiment illustrated in Fig. 5. Homogeneous Si(111)$\sqrt{3}\times\sqrt{3}$-Al surface was prepared by depositing ~0.25 ML of Al onto the Si(111)7×7 surface held at 700 °C [Fig. 5(a)]. Then, a certain amount of Ge was deposited onto this surface at RT followed by annealing. The transition from the $\sqrt{3}\times\sqrt{3}$ structure to the magic cluster array (α-7×7 phase) occurs at Ge coverage beyond ~0.4 ML and annealing temperature beyond ~350 °C. The forming magic cluster arrays are typically incomplete [Fig. 5(b)]; the cluster density amounts about 60% of its ideal value, which is two clusters per 7×7 unit cell. Simultaneously, the surplus Al agglomerates to form domains of the γ phase. The transition starts from the step edge on the upper terrace as shown in Fig. 5(c).

One can see that the γ phase is the most preferable and stable configuration in the Al/Ge$_x$Si$_{1-x}$(111) system. The tendency for its formation at the expense of the other Al-induced structures (e.g., at the expense of dissolution of the magic clusters in α-7×7 phase) enhances with increasing Ge coverage to 1.0 ML and beyond. At relatively low temperatures of around 550 °C, the patches of the diluted magic cluster arrays still preserve (plausibly, due the kinetic limitations), while at ~750 °C the surface comprises domains of the γ phase surrounded by the bare 7×7 reconstruction with scarce magic clusters on it. (Recall that Al coverage in the γ phase is ~0.65–0.75 ML, which is almost three times greater than the average value of 0.25 ML present on the surface.)

Summarizing the results of the LEED-STM observations, let us consider the general effect of Ge on the stability of the Al adsorption configurations on Si(111) surface. One can see that all the Al/Si(111) reconstructions can be subdivided into two groups. The first group combines the reconstructions made of Al adatoms ($\sqrt{3}\times\sqrt{3}$ and $\sqrt{7}\times\sqrt{7}$). The second group unifies the reconstructions containing Al in the substitutional sites of the Si(111) lattice (γ phase and α-7×7 phase). Note that the α-7×7 phase is attributed to the second group as each magic cluster is essentially a triangular domain of the Si-Al bilayer [see Fig. 1(c)].[29,30] In the pure Al/Si(111) system, the Al adatom appears to be more stable than the Al atom in the substitutional site, hence the irreversible transition from the α-7×7 phase to the $\sqrt{3}\times\sqrt{3}$ reconstruction upon heating beyond 600 °C. With increasing Ge content in the Si(111) substrate, stability of the substitutional configuration grows over the stability of the adatom configuration and the reconstructions of the second group (α-7×7 phase and γ phase) prevail over the adatomlike $\sqrt{3}\times\sqrt{3}$ reconstruction.

C. Al/Si(111) and Al/Ge(111): Density-functional theory calculations

To quantify the relative stability of the competitive Al adsorption configurations, we conducted first-principles calculations of their formation energies. As a starting point, we considered the pure Al/Si(111) and Al/Ge(111) systems, for which stability of the Al atom in the adatom and substitutional sites was evaluated. Results of the calculations are summarized in Table I. Here, the relative stability is compared within each material system and the energy of the adatom configuration is set to zero. For the Al/Si(111) system, the preference of the adatom configuration is evident; it is by 0.43 eV more stable than the substitutional configuration. This coincides with the experimental observations mentioned

TABLE I. Calculated relative formation energies of the adatom and substitutional configurations for Al atom at Si(111) and Ge(111) surfaces. Energies of the adatom configurations are taken as zero.

Configuration	ΔE in eV/(1×1 cell)
Al/Si(111) adatom	0.00
Al/Si(111) substitution	+0.43
Al/Ge(111) adatom	0.00
Al/Ge(111) substitution	+0.03

above. For the Al/Ge(111) system, the results of the calculations are not so unambiguous; the formation energy of both configurations appears to be the same within accuracy of the calculations. Thus, one could conclude that, in contrast to the Al/Si(111) system adatom configuration, the Al/Ge(111) system has, at a minimum, no preference over substitution configuration. As for the experiment, the adatomlike $\sqrt{3}\times\sqrt{3}$ reconstruction has never been observed on Ge(111) surface for any group-III adsorbates Al,[28] Ga,[31,32] and In,[33,34] but formation of the incommensurate reconstructions akin the Al/Si(111) γ phase have been detected for all of them.

D. α-7×7 phase at Al/Ge$_x$Si$_{1-x}$(111): Density-functional theory calculations

In this subsection, we consider the sequence of Si atom substitution for Ge in the α-7×7 phase. To set the stage, Fig. 6 illustrates notation used for the various Si sites in the α-7×7 phase. Note that in Fig. 6 a half unit cell is presented; hence, the whole number of equivalent sites in the full 7×7 unit cell is twice that seen in the figure. The Si sites are as follows:

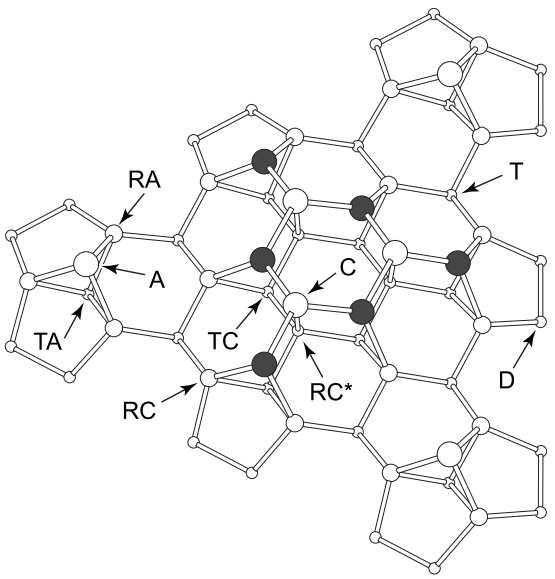

FIG. 6. Schematic illustrating various Si sites in the α-7×7 phase. Si atoms are shown by white circles and Al atoms by black circles. For indicated notation see the text.

(i) six Si corner adatoms (labeled A),
(ii) 18 Si rest-layer atoms to which six Si corner adatoms are bonded (labeled RA),
(iii) six Si T_4 atoms beneath six Si corner adatoms (labeled TA),
(iv) six Si atoms incorporated in two magic clusters (labeled C),
(v) 18 Si rest-layer atoms surrounding magic clusters, i.e., those to which Al atoms of the magic clusters are bonded (labeled RC),
(vi) six Si rest-layer atoms beneath Si atoms of the magic clusters (labeled RC*),
(vii) 12 Si T_4 atoms beneath Al atoms of the magic clusters (labeled TC),
(viii) 12 Si T_4 atoms in between magic clusters and Si corner adatoms (labeled T), and
(ix) 18 Si atoms constituting dimers (labeled D).

To describe the structure and composition of a particular Al/Ge$_x$Si$_{1-x}$(111)-α-7×7 phase, we indicate which Si atoms are substituted by Ge. For example, notation $A_6RA_{18}C_6$ is for the α-7×7 phase in which all corner Si adatoms A, all rest-layer atoms to which the adatoms are bonded RA, and all Si atoms incorporated in the magic clusters C are substituted by Ge [Fig. 8(b)].

Using density-functional theory calculations, formation energies were determined for 38 various configurations. The obtained results are summarized in Table II and Fig. 7 which show energies of the configurations as a function of the Ge coverage incorporated in the α-7×7 phase. In Table II, configurations are labeled according to the notation described above. In Fig. 7, the configurations are indicated by their numbers in Table II. For each Ge coverage several configurations have typically been evaluated of which the one having the lowest energy can be considered as the most plau-

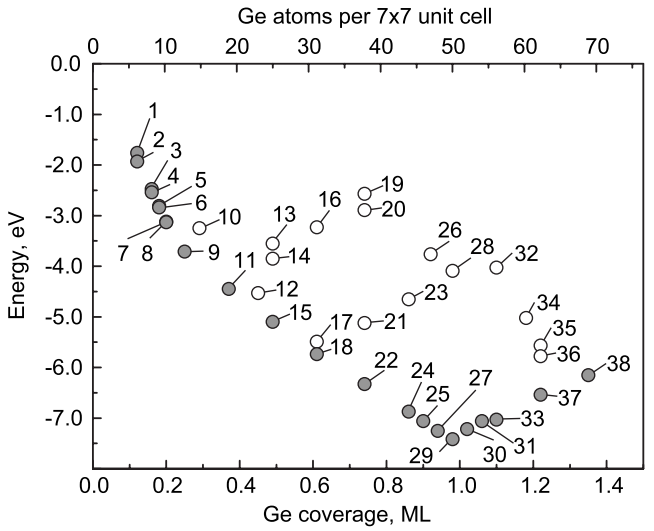

FIG. 7. Calculated formation energies for the various configurations of the Al/Ge$_x$Si$_{1-x}$(111)-α-7×7 phase as a function of Ge coverage. Energy of the Ge-free Al/Si(111)-α-7×7 phase is taken as zero. Configurations are indicated according to their numbers in Table II. Shaded dots correspond to the configurations forming the "reaction pathway" for the substitution of Si atoms by Ge in the α-7×7 phase.

TABLE II. Calculated formation energies for the various configurations of the Al/Ge_xSi_{1-x}(111)-α-7×7 phase. Energy of the Ge-free Al/Si(111)-α-7×7 phase is taken as zero.

Θ_{Ge}	Number	Configuration	Energy (eV)
0.12	1	C_6	−1.8
0.12	2	A_6	−1.9
0.16	3	A_2C_6	−2.5
0.16	4	A_6C_2	−2.5
0.18	5	A_3C_6	−2.8
0.18	6	A_6C_3	−2.8
0.20	7	A_4C_6	−3.1
0.20	8	A_6C_4	−3.1
0.25	9	A_6C_6	−3.7
0.29	10	$A_2RA_6C_6$	−3.3
0.37	11	$A_6RA_6C_6$	−4.5
0.45	12	$A_4RA_{12}C_6$	−4.5
0.49	13	C_6RC_{18}	−3.6
0.49	14	A_6RA_{18}	−3.9
0.49	15	$A_6RA_{12}C_6$	−5.1
0.61	16	$A_6RA_{18}TA_6$	−3.2
0.61	17	$A_6C_6RC_{18}$	−5.5
0.61	18	$A_6RA_{18}C_6$	−5.7
0.73	19	$C_6RC_{18}RC_6^{\star}TC_6$	−2.6
0.73	20	$A_6RA_{18}TA_6C_6$	−2.9
0.73	21	$A_6C_6RC_{18}RC_6^{\star}$	−5.1
0.73	22	$A_6RA_{18}C_6RC_6$	−6.3
0.86	23	$A_6C_6RC_{18}RC_6^{\star}TC_6$	−4.7
0.86	24	$A_6RA_{18}C_6RC_{12}$	−6.9
0.90	25	$A_6RA_{18}C_6RC_{14}$	−7.1
0.92	26	$A_6C_5RC_{16}RC_6^{\star}TC_{12}$	−3.8
0.94	27	$A_6RA_{18}C_6RC_{16}$	−7.3
0.98	28	$A_6RA_3C_5RC_{16}RC_6^{\star}TC_{12}$	−4.1
0.98	29	$A_6RA_{18}C_6RC_{18}$	−7.4
1.02	30	$A_6RA_{18}C_6RC_{18}RC_2^{\star}$	−7.2
1.06	31	$A_6RA_{18}C_6RC_{18}RC_4^{\star}$	−7.1
1.10	32	$A_6RA_{18}TA_6D_{12}T_{12}$	−4.0
1.10	33	$A_6RA_{18}C_6RC_{18}RC_6^{\star}$	−7.0
1.18	34	$A_4RA_{12}C_6RC_{18}RC_6^{\star}TC_{12}$	−5.0
1.22	35	$A_6RA_{12}C_6RC_{18}RC_6^{\star}TC_{12}$	−5.6
1.22	36	$A_6RA_{18}TA_6C_6D_{12}T_{12}$	−5.8
1.22	37	$A_6RA_{18}C_6RC_{18}RC_6^{\star}TC_6$	−6.5
1.35	38	$A_6RA_{18}C_6RC_{18}RC_6^{\star}TC_{12}$	−6.2

sible. Thus, a set of the lowest-energy configurations illustrates reaction pathway for the substitution of Si atoms by Ge in the α-7×7 phase. As one can see, the first Si atoms to be substituted are the most top ones, namely, Si corner adatoms A and Si atoms incorporated in the magic clusters C. Remarkably, the A_6 and C_6 configurations have almost similar energies with a slight preference (by ~0.2 eV) for the A_6 configuration. The energy difference for the "mixed" A_2C_6 and A_6C_2 (A_3C_6 and A_6C_3) configurations is still less. This

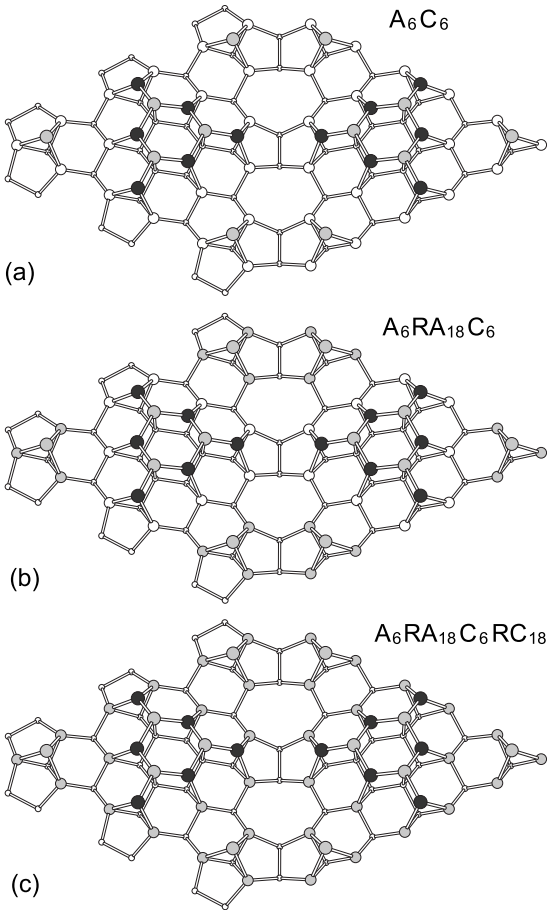

FIG. 8. Atomic configurations demonstrating the highest stability at given Ge coverage including (a) A_6C_6 at 0.24 ML of Ge, (b) $A_6RA_{18}C_6$ at 0.61 ML of Ge, and (c) $A_6RA_{18}C_6RC_{18}$ at 0.98 ML of Ge. The Si atoms substituted by Ge atoms are shaded.

stage is completed by developing the A_6C_6 configuration at 0.24 ML of Ge [Fig. 8(a)]. At the next stage, Si rest-layer atoms around corner Ge adatoms RA are substituted, leading to the $A_6RA_{18}C_6$ configuration with 0.61 ML of Ge [Fig. 8(b)]. Then, Si rest-layer atoms surrounding magic clusters RC become involved in the substitution process and the $A_6RA_{18}C_6RC_{18}$ is developed at 0.98 ML of Ge [Fig. 8(c)]. This configuration is believed to represent the global minimum for the Al/Ge_xSi_{1-x}(111)-α-7×7 phase as having the lowest energy among all the configurations tested in the present study. Substitution of the deeper Si atoms (e.g., $RC^{\star}$, TC, TA, etc.) with increasing Ge coverage beyond 1.0 ML results in the growing energy. Note that this result is in a principal agreement with the experimental data which indicate that, at relatively large Ge coverage, the magic clusters loose their enhanced stability and become replaced by a γ phase.

IV. CONCLUSION

In conclusion, using STM and LEED observations and density-functional calculations we have examined how adding Ge to Si(111) substrate affects the reconstructions formed

by adsorption of ~0.3 ML of Al onto the surface. It has been found that all the reconstructions typical for the pure Al/Si(111) system, $\sqrt{3}\times\sqrt{3}$, $\sqrt{7}\times\sqrt{7}$, magic cluster array (α-7$\times$7-phase), and γ phase, are preserved at the $Ge_xSi_{1-x}(111)$ surface but their relative stability alters dramatically. While in the pure Al/Si(111) system the Al adatom configuration is more stable than the Al substitutional configuration (hence, the irreversible transition of the α-7$\times$7 phase to the $\sqrt{3}\times\sqrt{3}$ reconstruction upon heating above 600 °C), adding Ge makes the Al substitutional configuration preferable over Al adatom configuration. Thus, by adding Ge to the $\sqrt{3}\times\sqrt{3}$-Al reconstruction, one can restore the α-7$\times$7 phase. The α-7$\times$7 phase in the $Al/Si_xGe_{1-x}(111)$ system possesses an enhanced thermal stability and persists almost up to the Al desorption temperature of ~800° that might be very useful for its applications, in particular, as a catalyst.[10] Results of the calculations allow us to track the sequential stages of the substitution of Si atoms by Ge in α-7$\times$7 together with the total-energy change. It has been found that Ge atoms substitute first the corner Si adatoms and Si atoms incorporated in the Al_6Si_3 magic clusters, then the rest-layer Si around Si adatoms followed by the rest-layer Si around the clusters.

ACKNOWLEDGMENTS

Part of this work was supported by the Russian Foundation for Basic Research (Grant No. 07-02-00650) and the Russian Federation Ministry of Education and Science (Grant No. 2007-3-1.3-07-01-352).

[1] V. G. Lifshits, A. A. Saranin, and A. V. Zotov, *Surface Phases on Silicon* (Wiley, Chichester, 1994).
[2] V. G. Lifshits, K. Oura, A. A. Saranin, and A. V. Zotov, in *Physics of Covered Solid Surfaces*, Landolt-Börnstein, New Series, Group III Vol. 42, 1st ed., edited by H. P. Bonzel (Springer-Verlag, Berlin, Heidelberg, New York, 2001), pp. 259–419.
[3] R. M. Tromp, Phys. Rev. B **47**, 7125 (1993).
[4] J. A. Carlisle, T. Miller, and T. C. Chiang, Phys. Rev. B **49**, 13600 (1994).
[5] F. Rosei, N. Motta, A. Sgarlata, G. Capellini, and F. Boscherini, Thin Solid Films **369**, 29 (2000).
[6] M. Kawamura, N. Paul, V. Cherepanov, and B. Voigtländer, Phys. Rev. Lett. **91**, 096102 (2003).
[7] B. Voigtländer, M. Kawamura, N. Paul, and V. Cherepanov, Thin Solid Films **464-465**, 185 (2004).
[8] D. V. Gruznev, D. A. Olyanich, D. N. Chubenko, A. V. Zotov, and A. A. Saranin, Phys. Rev. B **76**, 073307 (2007).
[9] Y. L. Wang, A. A. Saranin, A. V. Zotov, M. Y. Lai, and H. H. Chang, Int. Rev. Phys. Chem. **27**, 317 (2008).
[10] Z. Zhang, Q. Fu, H. Zhang, Y. Li, Y. Yao, D. Tan, and X. Bao, J. Phys. Chem. **111**, 13524 (2007).
[11] M. Bockstedte, A. Kley, J. Neugebauer, and M. Scheffler, Comput. Phys. Commun. **107**, 187 (1997).
[12] R. Car and M. Parrinello, Phys. Rev. Lett. **55**, 2471 (1985).
[13] D. M. Ceperley and B. J. Alder, Phys. Rev. Lett. **45**, 566 (1980).
[14] J. P. Perdew and A. Zunger, Phys. Rev. B **23**, 5048 (1981).
[15] D. R. Hamann, Phys. Rev. B **40**, 2980 (1989).
[16] M. Fuchs and M. Scheffler, Comput. Phys. Commun. **119**, 67 (1999).
[17] E. A. Khramtsova, A. V. Zotov, A. A. Saranin, S. V. Ryzhkov, A. B. Chub, and V. G. Lifshits, Appl. Surf. Sci. **82-83**, 576 (1994).
[18] V. G. Kotlyar, T. V. Kasyanova, E. N. Chukurov, A. V. Zotov, and A. A. Saranin, Surf. Sci. **545**, L779 (2003).
[19] A. V. Zotov, E. A. Khramtsova, S. V. Ryzhkov, A. A. Saranin, A. B. Chub, and V. G. Lifshits, Surf. Sci. **316**, L1034 (1994).
[20] J. J. Lander and J. Morrison, Surf. Sci. **2**, 553 (1964).
[21] K. Nishikata, K. Murakami, M. Yoshimura, and A. Kawazu, Surf. Sci. **269-270**, 995 (1992).
[22] Y. Sugawara, S. Orisaka, and S. Morita, Appl. Surf. Sci. **157**, 239 (2000).
[23] A. A. Saranin, V. G. Kotlyar, A. V. Zotov, T. V. Kasyanova, M. A. Cherevik, and V. G. Lifshits, Surf. Sci. **517**, 151 (2002).
[24] V. G. Kotlyar, A. V. Zotov, A. A. Saranin, T. V. Kasyanova, M. A. Cherevik, I. V. Pisarenko, and V. G. Lifshits, Phys. Rev. B **66**, 165401 (2002).
[25] J. Jia, J. Z. Wang, X. Liu, Q. K. Xue, Z. Q. Li, Y. Kawazoe, and S. B. Zhang, Appl. Phys. Lett. **80**, 3186 (2002).
[26] R. W. Li, S. Kusano, J. H. G. Owen, and K. Miki, Nanotechnology **17**, 2018 (2006).
[27] R. W. Li, J. H. G. Owen, S. Kusano, and K. Miki, Appl. Phys. Lett. **89**, 073116 (2006).
[28] W. Yang and F. Jona, Solid State Commun. **42**, 49 (1982).
[29] M. Y. Lai and Y. L. Wang, Phys. Rev. B **60**, 1764 (1999).
[30] S. F. Tsay, M. H. Tsai, M. Y. Lai, and Y. L. Wang, Phys. Rev. B **61**, 2699 (2000).
[31] M. Böhringer, P. Molinás-Mata, E. Artacho, and J. Zegenhagen, Phys. Rev. B **51**, 9965 (1995).
[32] J. Zegenhagen, P. Lyman, M. Böhringer, and M. Bedzyk, Phys. Status Solidi B **204**, 587 (1997).
[33] M. Böhringer and J. Zegenhagen, Surf. Sci. **327**, 248 (1995).
[34] Z. Gai, R. G. Zhao, Y. He, H. Ji, C. Hu, and W. S. Yang, Phys. Rev. B **53**, 1539 (1996).